


 Cite this: *RSC Adv.*, 2023, **13**, 23708


Received 2nd June 2023

Accepted 31st July 2023

DOI: 10.1039/d3ra03689h

rsc.li/rsc-advances

Spectral properties and self-reduction of Eu^{3+} to Eu^{2+} in aluminosilicate oxyfluoride glass

 Lei Liu, Xianying Shao, Zhenyuan Zhang, Jiayu Liu, Yuebo Hu * and Chaofeng Zhu*

Eu-doped aluminosilicate oxyfluoride glass prepared via a melt-quenching method was investigated using X-ray diffraction, absorption spectroscopy, X-ray fluorescence spectrometry, photoluminescence spectroscopy and fluorescence decay curves. We found that the reduction of Eu^{3+} to Eu^{2+} ions occurred in the glass prepared in air. The emission spectra showed that the intensity of $4f^65d \rightarrow 4f^7$ transition of Eu^{2+} ions varied with increasing incident beam wavelength. Meanwhile, the fluorescence lifetimes of Eu^{3+} : $^5\text{D}_0 \rightarrow ^7\text{F}_2$ monitored at 617 nm in the glass change with the variation of excitation wavelength. The energy transfer between Eu^{2+} and Eu^{3+} and the emission mechanisms of Eu^{2+} ions in the glass were also discussed.

1 Introduction

The photoluminescence (PL) of Eu-doped materials has been of extensive interest not only because of the excellent red emission of Eu^{3+} (ascribed to 4f–4f electronic forbidden transitions and the exhibiting of a series of highly bright and sharply narrow emissions),^{1–3} but because of the characteristic broadband emission of Eu^{2+} (attributed to inter-configurational $4f^65d \rightarrow 4f^7(^8\text{S}_{7/2})$ transitions and tuned from near-ultraviolet (UV) to red in different hosts).^{4–7} Impressively, due to stronger coupling to lattice vibrations (*i.e.*, the strong interaction of 5d electrons with the local crystal field in vicinity of Eu^{2+}), the unique electronic configuration of Eu^{2+} ($4f^7-4f^65d$) makes its luminescent properties sensitive to the coordination environment.^{8,9} This is why the emission of Eu^{2+} could present colorful emissions, which has recently made it a perfect candidate for color-tunable phosphors, such as the blue phosphor $\text{Mg}_2\text{Al}_4\text{Si}_5\text{O}_{18}:\text{Eu}^{2+}$,¹⁰ the green phosphor $\text{Rb}_3\text{M}(\text{Li}_3\text{SiO}_4)_4:\text{Eu}^{2+}$ (M = Rb or Na),¹¹ the green-to-yellowish-orange phosphor $\text{Cs}_2\text{MP}_2\text{O}_7:\text{Eu}^{2+}$ (M = Ba, Sr, and Ca),¹² the red phosphor $\text{CaS}:\text{Eu}$,¹³ and so on. Thus, Eu^{2+} -doped phosphors are of great technological interest for applications in white LED, optical thermometers, backlight displays, and X-ray storage, *etc.*^{10,11,14}

Aluminosilicate oxyfluoride glasses and glass-ceramics containing two kinds of anions (O^{2-} and F^-) with different valence electrons and different degrees of polarization is another kind of promising host for RE ions because they combine the advantages of the high mechanical strength of oxide glass and the low phonon energy of fluoride glass.^{14–16} Still, instead of the high-performance narrow-band emissions in Eu^{2+} -activated

phosphors for some special applications (*e.g.*, fluorescent illumination and X-ray intensifying panels),^{17,18} divalent europium ions generally emit only a broad band blue emission in vitreous hosts.^{19,20} In other words, the amorphous structure of glass, which resulting in a higher phonon energy, enhances the overlap of electronic orbit among energy levels in $4f^65d$ configuration, *i.e.*, the broad blue emission originates in the minor splitting energy of Eu 5d-band. However, the broad band emission of Eu^{2+} ions precisely makes it possible to generate tunable smooth spectra, especially warm white light-emitting, in single rare earth doped glass materials by regulating the emission intensity ratio between Eu^{3+} and Eu^{2+} .^{21,22} In addition, differing from the reduction process in phosphors synthesis (*i.e.*, in a strongly reducing atmosphere, *e.g.*, H_2/N_2 , *etc.*), $\text{Eu}^{3+} \rightarrow \text{Eu}^{2+}$ conversion in glass melting is fulfilled in air by adding a reducing agent into the glass composition (*e.g.*, Al) or adjusting the optical basicity (A_{th}) of the glass matrix (*i.e.*, to make the A_{th} value of base glass less than 0.585 by optimizing glass composition).^{3,12,23–25} Obviously, the reduction routes implemented in Eu-doped glasses are relatively convenient. All these mean that Eu-doped oxyfluoride glass materials have promising prospects in the quality lighting field.

In the present study, we developed an Eu-doped glass composition within the system $\text{SiO}_2\text{-Al}_2\text{O}_3\text{-BaF}_2\text{-Na}_2\text{O}$ containing both Eu^{3+} and Eu^{2+} ions, which was synthesized by partially reducing Eu^{3+} ions without using a reducing atmosphere and/or any reductant during the melting process. We performed multispectral excitation measurements (at the incident wavelength (λ_{ex}) ranging from 320 nm to 360 nm with an interval of 5 nm) and structure analysis to study the emission properties of Eu^{2+} ions in the glass sample. The energy transfer from Eu^{2+} to Eu^{3+} and the emission mechanisms of Eu^{2+} ions in the glass sample were discussed.

School of Materials Science and Engineering, Qilu University of Technology (Shandong Academy of Sciences), Jinan 250353, China. E-mail: huyb@qlu.edu.cn; cfzhu@qlu.edu.cn



2 Experimental

Aluminosilicate oxyfluoride glass with the nominal molar composition of $40\text{SiO}_2\text{-}25\text{Al}_2\text{O}_3\text{-}20\text{BaF}_2\text{-}15\text{Na}_2\text{O}\text{:}1\text{Eu}$ was synthesized by a melt-quenching method, using SiO_2 (99.99%, Aladdin), Al_2O_3 (99.99%, Aladdin), BaF_2 (99.99%, Aladdin), Na_2CO_3 (99.99%, Aladdin), and Eu_2O_3 (99.99%, Aladdin) as raw materials. All the chemicals were used as received without further purification. Accurately weighed 10 g per batch of raw materials were fully mixed and melted in a covered alumina crucible at 1723 K for 1 h. The melt was cast quickly into a metal mold with cover on copper-alloy plate of 573 K and finally cooled down to room temperature in air to obtain glass sample. It should be noted that the melting crucible for melting the glass batch was covered by another bigger alumina crucible to protect local atmosphere, *i.e.*, to reduce the volatilization loss of fluoride.^{26,27} The obtained glass sample was further polished to 1.5 mm in thickness for further optical measurements after annealed 10 h at 520 °C.

The amorphous characteristic of sample was determined with an X-ray diffraction (XRD, Shimadzu LabX XRD-6100) with $\text{Cu}/\text{K}\alpha$ ($\lambda = 1.540598 \text{ \AA}$) by short scanning in the 2θ range of 10–70° (2θ) at a scan rate of 6 ° min^{-1} . The UV/VIS/NIR absorption spectrum was recorded in the wavelength range from 200 to 450 nm using a Model U-4100 Spectrophotometer. The final product composition was measured using the X-ray Fluorescence Spectrometer (ZSX Primus II, Rigaku, JPN). The photoluminescence and decay curves were performed in FLS980 fluorescence spectrometer (FLS980, Edinburgh Instruments, UK) equipped with a Xe-lamp and μs flash lamp as excitation sources. All spectroscopic measurements were performed at room temperature.

3 Results and discussion

The X-ray diffraction pattern of the Eu-doped aluminosilicate oxyfluoride glass is shown in Fig. 1A. The characteristic amorphous halo (*i.e.*, a broad hump located at 27° (2θ)) and no diffraction peaks (*i.e.*, no crystalline phases precipitated from the sample) are observed in the spectrum. Fig. 1B shows the absorption spectrum of the Eu-doped as-prepared glass. It can be seen from this figure, a broad absorption band peaking at 275 nm and two absorption shoulders on the low-energy side, decomposed into three fitting bands using Gaussian function, are observed. The most remarkable band, peaking at 275 nm, is assigned to aluminosilicate oxyfluoride glass host absorption. The other two weaker absorption peaks could be attributed to the electronic transition of $4f^7 \rightarrow 4f^65d$, *i.e.*, the 5d orbital is split into two components t_{2g} (318 nm) and e_g (389 nm) by the crystal-field strength of the coordinates in the vicinity of Eu^{2+} ions.²⁸ In addition, the Eu^{3+} also shows an absorption peak in the range 388–396 nm, whereas the absorption due to the Eu^{3+} : f–f transitions in aluminosilicate glass is obscure owing to their small absorption coefficients.²⁸ It is noteworthy that, differing from the absorption spectra in Eu-doped phosphors (*i.e.*, where the absorption band of host and those of Eu^{2+} ions were obviously separated),^{12,29} the absorption bands of host and Eu^{2+} ions

are closely overlapping in the aluminosilicate oxyfluoride glass. In addition, this absorption band is not in agreement with Eu^{2+} absorption spectra in oxide aluminosilicate glasses, where a broad absorption band considered to contain only the e_g and t_{2g} splitting components of 5d orbitals of Eu^{2+} ions were observed, and believed that the sites of cubic symmetry with 8- and 12-fold coordination resulted in a splitting to e_g component at lower energy and t_{2g} component at higher energy.^{28,30} This result indicates that the phonon energy caused by lattice vibration of the aluminosilicate oxyfluoride host glass has extended into the bandgap of Eu^{2+} ions,^{31,32} which means the 5d energy level of the doped Eu^{2+} ions should be widen. Furthermore, IR spectra also manifests the multiple broad-band absorption peaks (Fig. 1C. 950 cm^{-1} : Si–O–Si, 690 cm^{-1} : Al–O, and 440 cm^{-1} : Si–O–Si and O–Si–O, *etc.*), meaning various energies (often referred to collectively as ‘phonon energy’) contained in glass. The broad bands will benefit the overlap of electronic orbit among energy levels in $4f^65d$ configuration of Eu^{2+} ions. This predicts that, compared to the emission spectra of Eu^{2+} in above-mentioned hosts, especially the phosphor hosts, a broader emission band of Eu^{2+} will be observed in the studied host glass, *i.e.*, the $40\text{SiO}_2\text{-}25\text{Al}_2\text{O}_3\text{-}20\text{BaF}_2\text{-}15\text{Na}_2\text{O}$ glass.

Fig. 2 exhibits the excitation spectra of Eu^{2+} and Eu^{3+} ions for Eu-doped aluminosilicate oxyfluoride glass. We can see from this figure that the 5d band of Eu^{2+} is observed in the excitation spectrum monitored at 471 nm. Furthermore, the broad excitation band (*i.e.*, the energy transfer Eu^{2+} : $^8\text{S}_{7/2} \rightarrow 5d$) can be fitted into two bands by Gaussian function, indicating that the 5d orbital of Eu^{2+} ions in the studied glass system is split to two components t_{2g} and e_g by its surrounding crystal field. At the same time, one can observe in this figure, two weaker excitation bands around 320 nm (just showing half peak because of a severe disturbance by the frequency-doubled excitation peak of FLS1000 fluorescence spectrometer used in this study) and 370 nm can also be distinguished in the excitation spectrum of Eu^{3+} ions. This indicates the possibility that energy transfer (ET) from Eu^{2+} ions 5d level to the Eu^{3+} ions 4f levels. Indeed, as Malchukova proved,²⁰ the overlap between the broad emission of Eu^{2+} ions and the various excitation bands of Eu^{3+} ions is observed in Fig. 3.

The down conversion luminescence observed in the Eu-doped $40\text{SiO}_2\text{-}25\text{Al}_2\text{O}_3\text{-}20\text{BaF}_2\text{-}15\text{Na}_2\text{O}$ as-prepared glass can be attributed to both Eu^{3+} and Eu^{2+} ions, as shown in Fig. 3. This result confirms therefore that trivalent europium ions have been partially reduced to divalent europium in this studied aluminosilicate oxyfluoride glass composition synthesized in air at high temperature. In other words, the broad blue-green emission with maximum at 470 nm undoubtedly belongs to the transition $4f^65d \rightarrow 4f^7$ of Eu^{2+} ions. However, in this work, no reducing atmosphere or agent is employed to promote the reduction of Eu^{3+} ions (Eu_2O_3 as the precursor material). Thus, the existence of Eu^{2+} ions in the present aluminosilicate oxyfluoride glass system obtained in normal atmospheric condition can be explained adopting optical basicity model proposed by Duffy and Ingram characterizing the glasses based on acid–base property.³³ Unlike

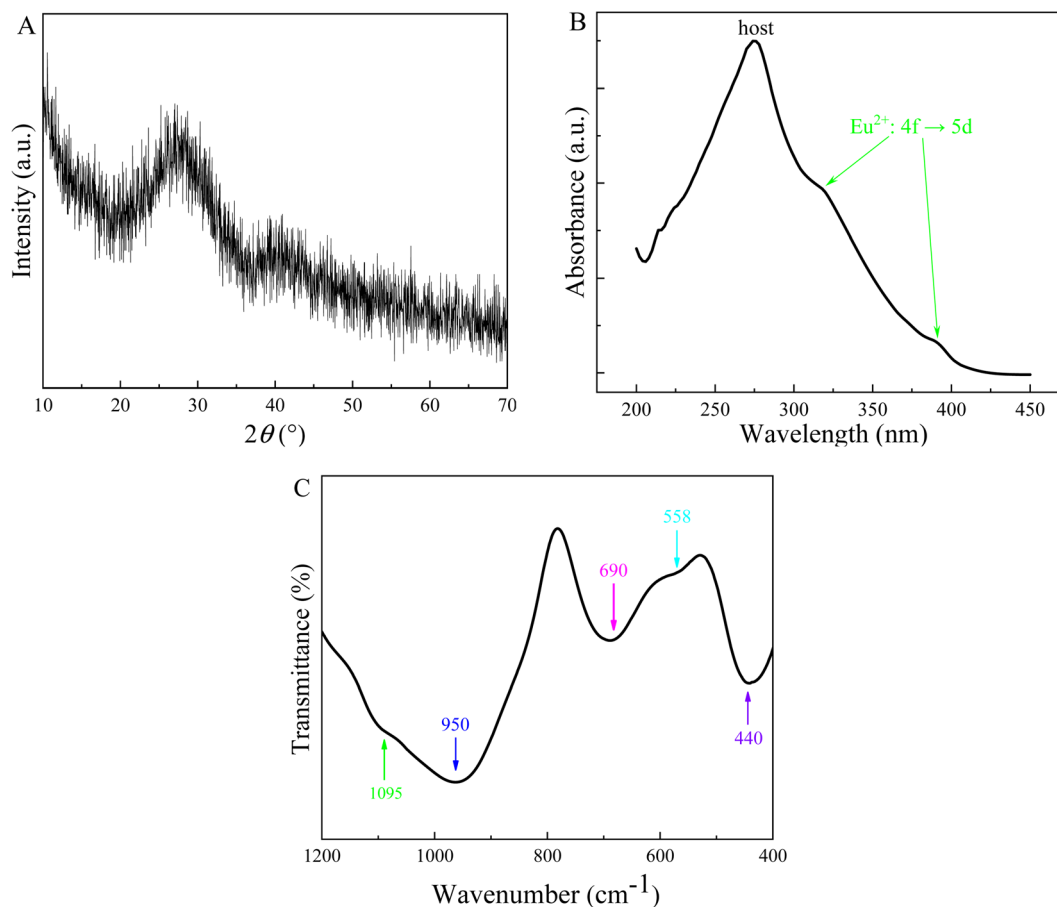


Fig. 1 XRD patterns spectrum (A), optical absorption spectrum (B) and IR spectra (C) for the Eu-doped $40\text{SiO}_2-25\text{Al}_2\text{O}_3-20\text{BaF}_2-15\text{Na}_2\text{O}$ glass. The broad absorption band in (B) contains two shoulders, indicating it could be deconvoluted into three Gaussian functions. IR spectra in (C) manifests multiple broad-band absorption peaks.

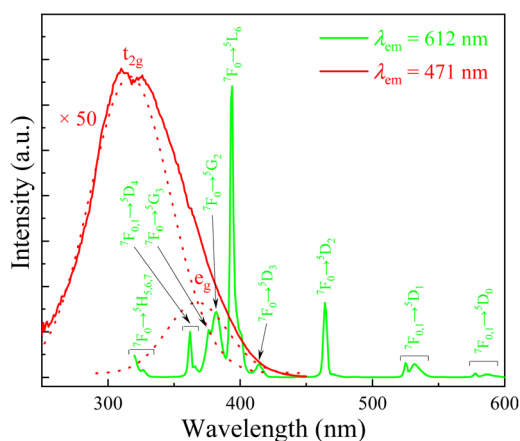


Fig. 2 Excitation spectra for Eu^{2+} ions (red line) and Eu^{3+} ions (green line) monitored at 471 and 612 nm, respectively, measured for the Eu-doped $40\text{SiO}_2-25\text{Al}_2\text{O}_3-20\text{BaF}_2-15\text{Na}_2\text{O}$ glass. The broad excitation band was deconvoluted to two Gaussian functions (dotted red lines). The excitation spectrum and its two Gaussian fitting bands were magnified 50 times in intensity (for interpretation of the references to color in this figure legend, the reader referred to the web version of this article).

the classical principle to elucidate the synthesis mechanism for europium monoxide (EuO) *via* calculating various thermodynamics parameters (*e.g.*, Gibbs free energy, configurational entropy, *etc.*) and analyzing the effect of high temperature on the reduction of $\text{Eu}^{3+} \rightarrow \text{Eu}^{2+}$,^{34,35} the optical basicity theory is fundamentally correlated to the chemical bonding in a solid and to the optical properties of a material through the polarizability of electron clouds around atoms (ions) by electromagnetic waves. Optical basicity of a glass is assumed to represent the average oxygen environment throughout the material. The optical property of glasses, *e.g.*, the reduction-oxidation of cations, can be used to predict through optical basicity concepts.^{36,37}

From the optical basicity concept, as the optical basicity of glass matrix is below a certain critical value (*i.e.*, critical value of 0.585), it favors the transformation of higher oxidation state to lower oxidation state for multivalent cation europium.²⁵ Considering equivalent mole fractions of constituent oxide or fluoride that contributes to the overall glass stoichiometry and their individual reported values of basicity along with number of oxygen or fluorine atoms, the optical basicity (\mathcal{A}_{th}) of the glass matrix is calculated using Duffy's empirical formula:

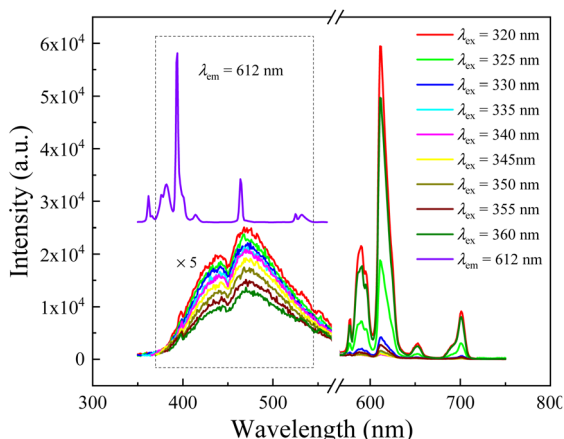


Fig. 3 Emission spectra for Eu^{2+} ions in dependence on excitation wavelength from 320 nm to 360 nm with an interval of 5 nm and excitation spectrum for Eu^{3+} ions (purple line) monitored at 612 nm, respectively, measured for Eu-doped $40\text{SiO}_2\text{-}25\text{Al}_2\text{O}_3\text{-}20\text{BaF}_2\text{-}15\text{Na}_2\text{O}$ as-prepared glass. The emission spectra bands at the wavelength range from 350 to 560 nm are magnified 5 times in intensity and show "holes" corresponding to Eu^{3+} ions absorption. Excitation spectrum of Eu^{3+} ions is vertically shifted to make comparison (for interpretation of the references to color in this figure legend, the reader referred to the web version of this article).

$$A_{\text{th}} = \frac{\sum_i x_i q_i A_i}{\sum_i x_i q_i} \quad (1)$$

where, q_i is the number of oxygen or fluorine atoms in the i th component oxide or fluoride, x_i is the i th component oxide or fluoride mole fraction, and A_i is the optical basicity of i th oxide or fluorides. Herein, fluorine in the glass composition can be volatile during the preparation of glass at high temperature, leading the final product composition being different from the nominal one as designed.³⁸ Thus, we used the X-ray fluorescence spectrometer to measure the glass matrix composition of the obtained sample. The obtained base glass composition is $37.66\text{SiO}_2\text{-}27.44\text{Al}_2\text{O}_3\text{-}17.34\text{BaF}_2\text{-}3.86\text{BaO}\text{-}13.70\text{Na}_2\text{O}$ (in mol%).

Based on the previous reports,^{39,40} the optical basicity values of oxide or fluoride are listed as the following: $A(\text{SiO}_2) = 0.48$, $A(\text{Al}_2\text{O}_3) = 0.6$, $A(\text{BaF}_2) = 0.50$, $A(\text{BaO}) = 1.15$, $A(\text{Na}_2\text{O}) = 1.15$. Using the Duffy's empirical formula, the optical basicity of the base glass is calculated to be 0.5864, which is very close to the critical optical basicity ($A_{\text{th}} = 0.585$). According to the theory proposed by Duffy, a higher optical basicity favors a higher valence state of the multivalence metal ions.⁴¹ This implies that it is more propitious to generation a lower valence ion, *i.e.*, Eu^{2+} , at lower optical basicity in this work. In addition, Z. Y. Lin *et al.* reported the self-reduction of Eu^{3+} to Eu^{2+} in a kind of aluminosilicate glass with the optical basicity of 0.59.¹⁴ They proposed that the structures of aluminosilicate glass play an important role in the reduction of Eu^{3+} ions, which changes the critical optical basicity value under the special chemical environment. In the present study, the base glass composition also contains SiO_2 and Al_2O_3 . Thus, the formation of Eu^{2+} is realized in the present glass.

Seen from Fig. 3, the emission intensity of Eu^{2+} decreases slightly in turn with the increasing excitation wavelength from 320 to 360 nm (*i.e.*, the wavelength range between the fitting peaks of t_{2g} and e_g for the 5d energy level of Eu^{2+} ions). It can be attributed to the reduced energy transfer capacity of $^8\text{S}_{7/2}$ level, directly leading to a reducing luminescence efficiency, as the incident light deviates from the peak of excitation band for Eu^{2+} ions monitored at 471 nm. However, the emission intensity of Eu^{3+} ions in the red wavelength range shows a variation trend, *i.e.*, it decreases before increases with the increasing incident light wavelength in the studied excitation wavelength range (320–360 nm). Despite the possibility of energy transfer from Eu^{2+} to Eu^{3+} exists, as mentioned above, the emission of Eu^{2+} ions is so weak that the transferred energy is faint. Thus, the intenser luminescence of Eu^{3+} excited under 320, 325 and 360 nm, respectively, can be ascribe to the notable overlap between incident to the excitation transition of Eu^{3+} : $^7\text{F}_0 \rightarrow ^5\text{H}_{5,6,7}$ and $^7\text{F}_{0,1} \rightarrow ^5\text{D}_4$. Whereas, the rest weaker luminescence of Eu^{3+} may be mainly related to the ET from Eu^{2+} to Eu^{3+} ions, especially the emission spectra under 335–355 nm excitation, because that no excitation band is shown in this wavelength range for Eu^{3+} ions shown as in Fig. 2. Moreover, this result falls in line with the energy transfer hypothesis in the section of excitation analysis, *i.e.*, the ET from Eu^{2+} ions 5d level to the Eu^{3+} ions 4f levels.

Fluorescence decay analysis is very useful for understanding the mechanism of rare earth luminescence, *e.g.*, energy transfer and quenching behavior *etc.* Fig. 4 shows the decay curves of Eu^{3+} (monitored at $\lambda_{\text{em}} = 617$ nm) in the aluminosilicate oxy-fluoride as-prepared glass under multispectral excitation at 320, 325, 330, 335, 340, 345, 350, 355, 360 nm, respectively. All the decay curves are fitted by a double exponential decay function with time constant parameters (ExpDec2) in Origin software using the below given expression:⁴²

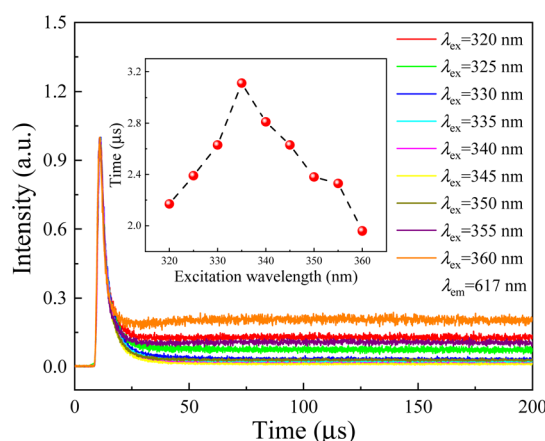


Fig. 4 Room-temperature luminescence decay curves of the emission Eu^{3+} : $^5\text{D}_0 \rightarrow ^7\text{F}_2$ at 617 nm excited by multispectral from 320 to 360 nm with an interval of 5 nm. All curves are normalized to make comparison. Inset: the dependence of decay lifetimes (τ) on excitation wavelength (λ_{ex}). The red spheres in the inset refer to the fluorescence lifetimes of Eu^{3+} : $^5\text{D}_0$ in the glass sample. The dashed curves are guide for eyes to show the nonmonotonic change of τ with increasing λ_{ex} .

$$I(t) = A_1 \exp\left(-\frac{t}{\tau_1}\right) + A_2 \exp\left(-\frac{t}{\tau_2}\right) \quad (2)$$

where $I(t)$ is the emission intensity at time t . A_1 and A_2 are the decay constants. τ_1 and τ_2 are the lifetimes of the two channels contributing to the decay processes. The average fluorescence lifetime (τ) is estimated as follows:

$$\tau = \frac{A_1 \tau_1^2 + A_2 \tau_2^2}{A_1 \tau_1 + A_2 \tau_2} \quad (3)$$

Interestingly, τ evolves non-monotonically with λ_{ex} as seen in the inset of Fig. 4. With increasing the excitation light wavelength, the fluorescence time first increases from 2.2 to 3.1 μs , and then decreases to 2.0 μs . This result confirms therefore that the emission mechanism of Eu^{3+} ions in the studied aluminosilicate oxyfluoride as-prepared glass changes with incident beam, *i.e.*, the faster decay (*e.g.*, excited at 320 and 325 nm) may relate to excited state absorption, and the slower decay (*e.g.*, excited at 355 and 360 nm) can be put down to energy transfer. This implies that the excitation process is faster than the energy transfer for Eu^{3+} ions in the studied glass system. The mechanism of energy transfer from Eu^{2+} : 5d to the Eu^{3+} : 4f is similar to that described in^{20,28}, *i.e.*, the excited in $4f^65d$ (e_g) state of Eu^{2+} ions transfers the energy by means of non-radiative transition $4f^65d$ (e_g) \rightarrow $^8S_{7/2}$ to the ground state resulting in the excitation of 5D_0 level of Eu^{3+} ions. We also observed another evidence for the energy transfer from Eu^{2+} to Eu^{3+} ions by analyzing the excitation spectrum (Fig. 2) and emission spectra (Fig. 3) of Eu^{2+} , *i.e.*, the discontinuous peaks, especially at 320 nm in the excitation band monitored at 471 nm. This type of effect where band emission is suppressed only at the position of RE absorption lines is known to be characteristic of resonant radiative energy transfer, *i.e.*, the reabsorption mechanism.^{43,44} Significantly, being inconsistent with the results of Jiménez *et al.*,⁴⁴ the “holes” on the emission bands of Eu^{2+} don't directly correspond the Eu^{3+} ions absorption peaks on its excitation band, as shown in Fig. 3. The possible reason may be the strong phonon energy of the aluminosilicate oxyfluoride host glass as observed in the above-mentioned absorption and IR analyses, *i.e.*, implying the occurrence of multi-phonon relaxation.

The effect of varying incident beam wavelength (λ_{ex} from 320 to 360 nm) on the luminescence color in Eu-doped aluminosilicate oxyfluoride as-prepared glass is displayed in Fig. 5. The luminescence color can be finely tuned by changing the excitation wavelength, corresponding CIE coordinates vary from yellowish pink (0.5422, 0.3369), warm white light (0.3845, 0.2895), to greenish blue (0.2016, 0.247).

Surprisingly, we observed the heterogeneous distribution of Eu^{2+} ions in the studied Eu-doped glass system by analyzing the emission spectra of the other side of sample shown as in Fig. 6, *i.e.*, a photoluminescence increases before decreases with the increasing incident light wavelength from 330–360 nm which is contrary to that shown in Fig. 3. The phenomenon may be related to the variation of the local environment of Eu^{2+} ions. In other words, the results indicate that the phase separation has occurred in the studied glass. That is that the rich fluorine phase with

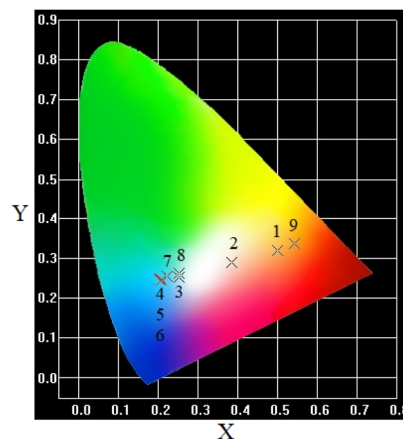


Fig. 5 Dependence of CIE chromaticity diagram on excitation wavelength for the Eu-doped $40\text{SiO}_2\text{-}25\text{Al}_2\text{O}_3\text{-}20\text{BaF}_2\text{-}15\text{Na}_2\text{O}$ glass. The numbers 1 to 9 represent the chromaticity coordinates under 320 to 360 nm excitation (for interpretation of the references to color in this figure legend, the reader referred to the web version of this article).

a lower optical basicity has emerged from the interpenetrating oxide phase. As mentioned above, the low optical basicity promoted the reduction from Eu^{3+} to Eu^{2+} , *i.e.*, the concentration of Eu^{2+} in rich fluoride is higher than that in dominant oxide phase. This is why the intensity of Eu^{2+} in Fig. 6 is obviously stronger than those in Fig. 3. The high symmetry properties of fluoride increase the splitting degree. Thus, the luminescence mechanism of Eu^{2+} ions under 330–360 nm excitation also changes along with it.

As using 330, 335, and 340 nm to excite the sample, the component of 5d level captured transition electron is e_g state, and the larger the wavelength of incident light, the closer the incident excitation energy is to the peak of e_g state. Thus, the emission intensity of Eu^{2+} ions increases with the enhancing excitation wavelength. But, as the incident light wavelength increases

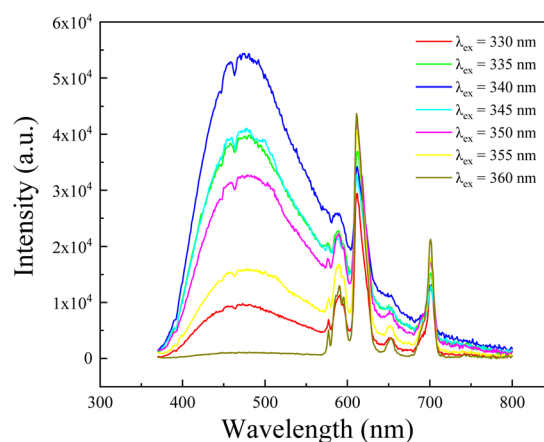


Fig. 6 Emission spectra for Eu^{2+} ions in dependence on excitation wavelength from 330 nm to 360 nm with an interval of 5 nm, respectively, measured for the Eu-doped $40\text{SiO}_2\text{-}25\text{Al}_2\text{O}_3\text{-}20\text{BaF}_2\text{-}15\text{Na}_2\text{O}$ glass (for interpretation of the references to color in this figure legend, the reader referred to the web version of this article).

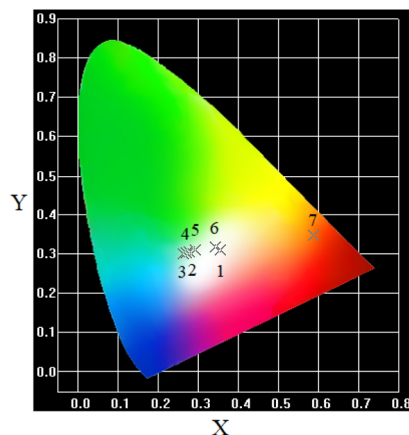


Fig. 7 Dependence of CIE chromaticity diagram on excitation wavelength for the Eu-doped $40\text{SiO}_2\text{-}25\text{Al}_2\text{O}_3\text{-}20\text{BaF}_2\text{-}15\text{Na}_2\text{O}$ glass. The numbers 1 to 7 represent the chromaticity coordinates under 330 to 360 nm excitation (for interpretation of the references to color in this figure legend, the reader referred to the web version of this article).

further, excitation electrons jump into t_{2g} state. Then, as mentioned above, the incident light from 340 to 360 nm deviates from the peak of excitation band. So, the emission intensity of Eu^{2+} ions decreases with the enhancing excitation wavelength. The increase in relative concentration of Eu^{2+} ions leads to richer white light emission shown as in Fig. 7. These results indicate that, just by Eu-individually-doped aluminosilicate oxyfluoride glass, various color emissions can be achieved, and the sample has extensive application prospect in solid-state light devices.

4 Conclusions

Eu-doped aluminosilicate oxyfluoride glasses have been prepared by the melt-quenching method. In the glass prepared in the air condition, the reduction of Eu^{3+} to Eu^{2+} ions occurred in the air condition. It is confirmed that the presence of significant amount fluoride in the glass composition is critical to promote this reduction process due to it causes the decrease of optical basicity for the studied glass system. With the increasing incident light wavelength (in the studied excitation wavelength range 320–360 nm), the emission intensity of Eu^{3+} ions decreases before increases in the red wavelength range. At the same time, it was noticed that the fluorescence time first increases before decreases. In addition, the heterogeneous distribution of Eu^{2+} ions due to phase separation is observed in the studied luminescence glass system. The results indicate that the spectral properties depend on the excitation mode. The colorful emission of Eu-individual-doped aluminosilicate oxyfluoride glasses may bring potential applications in light-emitting diode systems, three-dimensional displays, etc.

Author contributions

Lei Liu: investigation, writing – original draft. Xianying Shao: investigation, writing – original draft. Zhenyuan Zhang:

investigation, original draft. Jiayu Liu: investigation, original draft. Yuebo Hu: supervision, data curation, methodology, investigation, writing – original draft – review & editing, validation. Chaofeng Zhu: supervision, data curation, methodology, writing – review & editing, validation.

Conflicts of interest

The authors declare that they have no known competing financial interests or personal relationships that could have appeared to influence the work reported in this paper.

Acknowledgements

This work is supported by the National Natural Science Foundation of China (No. 61368007), the Natural Science Foundation of Shandong Province (Grant No. ZR2019MEM053).

References

- R. Klement, K. Drdlíková, M. Kachlík, D. Drdlík, D. Galusek and K. Maca, Photoluminescence and optical properties of $\text{Eu}^{3+}/\text{Eu}^{2+}$ -doped transparent Al_2O_3 ceramics, *J. Eur. Ceram. Soc.*, 2021, **41**(9), 4896–4906, DOI: [10.1016/j.jeurceramsoc.2021.03.029](https://doi.org/10.1016/j.jeurceramsoc.2021.03.029).
- G. Blasse and B. C. Grabmaier, *Luminescence Materials*, Springer, Berlin, 1994.
- Y. D. Ma, X. S. Peng, M. Z. Fei, W. N. Zhang, L. M. Teng, F. F. Hu, R. F. Wei and H. Guo, Adjustable white luminescence and high thermal stability in $\text{Eu}^{2+}/\text{Eu}^{3+}/\text{Tb}^{3+}/\text{Al}$ co-doped aluminosilicate oxyfluoride glass, *J. Alloys Compd.*, 2020, **846**, 156435, DOI: [10.1016/j.jallcom.2020.156435](https://doi.org/10.1016/j.jallcom.2020.156435).
- F. Liu, J. D. Budai, X. F. Li, J. Z. Tischler, J. Y. Howe, C. J. Sun, R. S. Meltzer and Z. W. Pan, New Ternary Europium Aluminate Luminescent Nanoribbons for Advanced Photonics, *Adv. Funct. Mater.*, 2013, **23**(16), 1998–2006, DOI: [10.1002/adfm.201202539](https://doi.org/10.1002/adfm.201202539).
- T. Hu, Y. Gao, M. S. Molokeev, Z. G. Xia and Q. Y. Zhang, Eu^{2+} Stabilized at Octahedrally Coordinated Ln^{3+} Site Enabling Red Emission in $\text{Sr}_3\text{LnAl}_2\text{O}_{7.5}$ ($\text{Ln} = \text{Y}$ or Lu) Phosphors, *Adv. Opt. Mater.*, 2021, **9**(9), 2100077, DOI: [10.1002/adom.202100077](https://doi.org/10.1002/adom.202100077).
- G. J. Gao, S. Krolkowski, M. Y. Peng and L. Wondraczek, Tailoring super-broad photoluminescence from Eu^{2+} and dual-mode $\text{Eu}^{2+}/\text{Eu}^{3+}$ -doped alkaline earth aluminoborate glasses through site-similarity and ligand acidity, *J. Lumin.*, 2016, **180**, 234–240, DOI: [10.1016/j.jlumin.2016.08.025](https://doi.org/10.1016/j.jlumin.2016.08.025).
- P. Dorenbos, Energy of the first $4f^7 \rightarrow 4f^65d$ transition of Eu^{2+} in inorganic compounds, *J. Lumin.*, 2003, **104**(4), 239–260, DOI: [10.1016/S0022-2313\(03\)00078-4](https://doi.org/10.1016/S0022-2313(03)00078-4).
- S. S. Liang, P. P. Dang, G. G. Li, Y. Wei, Y. Wei, H. Z. Lian and J. Lin, New Insight for Luminescence Tuning Based on Interstitial Sites Occupation of Eu^{2+} in $\text{Sr}_3\text{Al}_{2-x}\text{Si}_x\text{O}_{5-x}\text{N}_x\text{Cl}_2$ ($x = 0\text{-}0.4$), *Adv. Opt. Mater.*, 2018, **6**(22), 1800940, DOI: [10.1002/adom.201800940](https://doi.org/10.1002/adom.201800940).

- 9 Y. Pan, X. Xie, Q. Huang, C. Gao, Y. Wang, L. Wang, B. Yang, H. Su, L. Huang and W. Huang, Inherently $\text{Eu}^{2+}/\text{Eu}^{3+}$ Codoped Sc_2O_3 Nanoparticles as High-Performance Nanothermometers, *Adv. Mater.*, 2018, **30**(14), 1705256, DOI: [10.1002/adma.201705256](https://doi.org/10.1002/adma.201705256).
- 10 D. Stefańska and P. J. Dereń, High Efficiency Emission of Eu^{2+} Located in Channel and Mg-Site of $\text{Mg}_2\text{Al}_4\text{Si}_5\text{O}_{18}$ Cordierite and Its Potential as a Bi-Functional Phosphor toward Optical Thermometer and White LED Application, *Adv. Opt. Mater.*, 2020, **8**(22), 2001143, DOI: [10.1002/adom.202001143](https://doi.org/10.1002/adom.202001143).
- 11 M. Liao, Q. Wang, Q. M. Lin, M. X. Xiong, X. Zhang, H. F. Dong, Z. P. Lin, M. R. Wen, D. Y. Zhu, Z. F. Mu and F. G. Wu, Na Replaces Rb towards High-Performance Narrow-Band Green Phosphors for Backlight Display Applications, *Adv. Opt. Mater.*, 2021, **9**(17), 2100465, DOI: [10.1002/adom.202100465](https://doi.org/10.1002/adom.202100465).
- 12 Y. Wei, Z. Y. Gao, S. W. Liu, S. T. Chen, G. C. Xing, W. Wang, P. P. Dang, A. A. A. Kheraif, G. G. Li and J. Lin, Highly Efficient Green-to-Yellowish-Orange Emitting Eu^{2+} -Doped Pyrophosphate Phosphors with Superior Thermal Quenching Resistance for w-LEDs, *Adv. Opt. Mater.*, 2020, **8**(6), 1901859, DOI: [10.1002/adom.201901859](https://doi.org/10.1002/adom.201901859).
- 13 J. N. Spencer, D. Merrikin, S. J. A. Pope, D. J. Morgan, N. Carthey and D. M. Murphy, CW EPR Investigation of Red-Emitting $\text{CaS}:\text{Eu}$ Phosphors: Rationalization of Local Electronic Structure, *Adv. Opt. Mater.*, 2020, **8**(22), 2001241, DOI: [10.1002/adom.202001241](https://doi.org/10.1002/adom.202001241).
- 14 Z. Y. Lin, H. D. Zeng, Y. F. Yang, X. L. Liang, G. R. Chen and L. Y. Sun, The Effect of Fluorine Anions on the Luminescent Properties of Eu -Doped Oxyfluoride Aluminosilicate Glasses, *J. Am. Ceram. Soc.*, 2010, **93**(10), 3095–3098, DOI: [10.1111/j.1551-2916.2010.04067.x](https://doi.org/10.1111/j.1551-2916.2010.04067.x).
- 15 Y. B. Hu, R. J. Dou and J. B. Qiu, Spectroscopic properties and energy transfers in $\text{Tb}^{3+}/\text{Ho}^{3+}/\text{Yb}^{3+}$ tri-doped oxyfluoride silicate glasses, *J. Non-Cryst. Solids*, 2015, **420**, 12–16, DOI: [10.1016/j.jnoncrsol.2015.04.007](https://doi.org/10.1016/j.jnoncrsol.2015.04.007).
- 16 Y. B. Hu, J. B. Qiu, Z. G. Song, Z. W. Yang, Y. Yang, D. C. Zhou, Q. Jiao and C. S. Ma, Spectroscopic properties of $\text{Tm}^{3+}/\text{Er}^{3+}/\text{Yb}^{3+}$ co-doped oxyfluorogermanate glasses containing silver nanoparticles, *J. Lumin.*, 2014, **145**, 512–517, DOI: [10.1016/j.jlumin.2013.08.022](https://doi.org/10.1016/j.jlumin.2013.08.022).
- 17 K. Takahashi, Progress in Science and Technology on Photostimulable $\text{BaFX}:\text{Eu}^{2+}$ ($\text{X} = \text{Cl}, \text{Br}, \text{I}$) and Imaging Plates, *J. Lumin.*, 2002, **100**(1–4), 307–315, DOI: [10.1016/S0022-2313\(02\)00447-7](https://doi.org/10.1016/S0022-2313(02)00447-7).
- 18 D. Dutzler, M. Seibald, D. Baumann and H. Huppertz, Alkali Lithosilicates: Renaissance of a Reputable Substance Class with Surprising Luminescence Properties, *Angew. Chem., Int. Ed.*, 2018, **57**(41), 13676–13680, DOI: [10.1002/anie.201808332](https://doi.org/10.1002/anie.201808332).
- 19 X. Y. Sun, X. C. Le, Z. H. Xiao, X. H. Shi, W. F. Wang, Z. F. Hu, Q. M. Yang, R. F. Wei and H. Guo, Self-reduction of Eu^{3+} to Eu^{2+} in europium-doped $\text{Li}_2\text{B}_4\text{O}_7$ glass prepared in air, *J. Am. Ceram. Soc.*, 2020, **103**(5), 3119–3125, DOI: [10.1111/jace.17012](https://doi.org/10.1111/jace.17012).
- 20 E. Malchukova and B. Boizot, Reduction of Eu^{3+} to Eu^{2+} in aluminoborosilicate glasses under ionizing radiation, *Mater. Res. Bull.*, 2010, **45**(9), 1299–1303, DOI: [10.1016/j.materresbull.2010.04.027](https://doi.org/10.1016/j.materresbull.2010.04.027).
- 21 T. K. Pietrzak, A. Gołębowska, J. Płachta, M. Jarczewski, J. Ryl, M. Wasiucionek and J. E. Garbarczyk, Photoluminescence of partially reduced $\text{Eu}^{2+}/\text{Eu}^{3+}$ active centers in a $\text{NaF}-\text{Al}_2\text{O}_3-\text{P}_2\text{O}_5$ glassy matrix with tunable smooth spectra, *J. Lumin.*, 2019, **208**, 322–326, DOI: [10.1016/j.jlumin.2018.12.060](https://doi.org/10.1016/j.jlumin.2018.12.060).
- 22 Y. Gao, S. Murai, K. Shinozaki, J. B. Qiu and K. Tanaka, Phase-Selective Distribution of Eu^{2+} and Eu^{3+} in Oxide and Fluoride Crystals in Glass-Ceramics for Warm White-Light-Emitting Diodes, *ACS Appl. Electron. Mater.*, 2019, **1**(6), 961–971, DOI: [10.1021/acsaelm.9b00129](https://doi.org/10.1021/acsaelm.9b00129).
- 23 J. Yan, L. X. Ning, Y. C. Huang, C. M. Liu, D. J. Hou, B. B. Zhang, Y. Huang, Y. Tao and H. B. Liang, Luminescence and electronic properties of $\text{Ba}_2\text{MgSi}_2\text{O}_7:\text{Eu}^{2+}$: a combined experimental and hybrid density functional theory study, *J. Mater. Chem. C*, 2014, **2**(39), 8328–8332, DOI: [10.1039/c4tc01332h](https://doi.org/10.1039/c4tc01332h).
- 24 Y. Gao, J. B. Qiu and D. C. Zhou, Investigation of optical properties: Eu with Al codoping in aluminum silicate glasses and glass-ceramics, *J. Am. Ceram. Soc.*, 2017, **100**(7), 2901–2913, DOI: [10.1111/jace.14807](https://doi.org/10.1111/jace.14807).
- 25 K. Biswas, S. Balaji, D. Ghosh, A. D. Sontakke and K. Annapurna, Near-infrared frequency down-conversion and cross-relaxation in $\text{Eu}^{2+}/\text{Eu}^{3+}-\text{Yb}^{3+}$ doped transparent oxyfluoride glass and glass-ceramics, *J. Alloys Compd.*, 2014, **608**, 266–271, DOI: [10.1016/j.jallcom.2014.04.126](https://doi.org/10.1016/j.jallcom.2014.04.126).
- 26 Y. B. Hu, S. W. Qiu, Y. Gao and J. B. Qiu, Crystallization and spectroscopic properties in Er^{3+} doped oxyfluorogermanate glass ceramics containing Na, *Opt. Mater.*, 2015, **45**, 82–86, DOI: [10.1016/j.optmat.2015.03.014](https://doi.org/10.1016/j.optmat.2015.03.014).
- 27 Y. B. Hu, X. Y. Shao, Z. Y. Wang, X. L. Xu, X. J. Han, H. Z. Tao and Y. Z. Yue, $\text{BaAl}_2\text{Si}_2\text{O}_8$ polymorphs and a novel reversible transition of BaAlF_5 in supercooled oxyfluoride aluminosilicate liquids, *J. Eur. Ceram. Soc.*, 2021, **41**(14), 7282–7287, DOI: [10.1016/j.jeurceramsoc.2021.07.021](https://doi.org/10.1016/j.jeurceramsoc.2021.07.021).
- 28 M. Nogami, T. Yamazaki and Y. Abe, Fluorescence properties of Eu^{3+} and Eu^{2+} in $\text{Al}_2\text{O}_3-\text{SiO}_2$ glass, *J. Lumin.*, 1998, **78**(1), 63–68, DOI: [10.1016/S0022-2313\(97\)98281-8](https://doi.org/10.1016/S0022-2313(97)98281-8).
- 29 X. T. Li, P. L. Li, C. J. Liu, L. Zhang, D. J. Dai, Z. H. Xing, Z. P. Yang and Z. J. Wang, Tuning the luminescence of $\text{Ca}_9\text{La}(\text{PO}_4)_7:\text{Eu}^{2+}$ via artificially inducing potential luminescence centers, *J. Mater. Chem. C*, 2019, **7**(46), 14601–14611, DOI: [10.1039/c9tc04828f](https://doi.org/10.1039/c9tc04828f).
- 30 M. Nogami and Y. Abe, Enhanced emission from Eu^{2+} ions in sol-gel derived $\text{Al}_2\text{O}_3-\text{SiO}_2$ glasses, *Appl. Phys. Lett.*, 1996, **69**(25), 3776–3778, DOI: [10.1063/1.116995](https://doi.org/10.1063/1.116995).
- 31 Y. B. Hu, Y. Shen, C. F. Zhu, S. J. Liu, H. Liu, Y. F. Zhang and Y. Z. Yue, Optical bandgap and luminescence in Er^{3+} doped oxyfluoro-germanate glass-ceramics, *J. Non-Cryst. Solids*, 2021, **555**, 120533, DOI: [10.1016/j.jnoncrsol.2020.120533](https://doi.org/10.1016/j.jnoncrsol.2020.120533).
- 32 G. V. Prakash, Absorption spectral studies of rare earth ions (Pr^{3+} , Nd^{3+} , Sm^{3+} , Dy^{3+} , Ho^{3+} and Er^{3+}) doped in NASICON

- type phosphate glass, $\text{Na}_4\text{AlZnP}_3\text{O}_{12}$, *Mater. Lett.*, 2000, **46**(1), 15–20, DOI: [10.1016/S0167-577X\(00\)00135-X](https://doi.org/10.1016/S0167-577X(00)00135-X).
- 33 J. A. Duffy and M. D. Ingram, An interpretation of glass chemistry in terms of the optical basicity concept, *J. Non-Cryst. Solids*, 1976, **21**(3), 373–410, DOI: [10.1016/0022-3093\(76\)90027-2](https://doi.org/10.1016/0022-3093(76)90027-2).
- 34 A. S. Borukhovich and A. V. Troshin, Methods of Synthesis of Europium Monoxide, in *Europium Monoxide*, Springer Series in Materials Science, 2018, 265, pp. 37–67, DOI: [10.1007/978-3-319-76741-3_2](https://doi.org/10.1007/978-3-319-76741-3_2).
- 35 G. J. McCarthy and W. B. White, On the stabilities of the lower oxides of the rare earths, *J. less-common met.*, 1970, **22**(4), 409–417, DOI: [10.1016/0022-5088\(70\)90128-1](https://doi.org/10.1016/0022-5088(70)90128-1).
- 36 Z. G. Song, D. C. Zhou, Z. W. Yang, Z. Y. Yin, R. F. Wang, J. H. Shang, K. Lou, Y. Y. Xu, Y. B. Hu and J. B. Qiu, Correlation between optical basicity and properties of broadband infrared fluorescence of bismuth-doped germanate glasses, *J. Chin. Ceram. Soc.*, 2010, **38**(11), 2133–2137.
- 37 K. G. F. Baucke and A. J. Duffy, The effect of basicity on redox equilibria in molten glasses, *Phys. Chem. Glasses*, 1991, **32**, 211–218.
- 38 C. Bocker, S. Bhattacharyya, T. Höche and C. Rüssel, Size distribution of BaF_2 nanocrystallites in transparent glass ceramics, *Acta Mater.*, 2009, **57**(20), 5956–5963, DOI: [10.1016/j.actamat.2009.08.021](https://doi.org/10.1016/j.actamat.2009.08.021).
- 39 J. A. Duffy, A common optical basicity scale for oxide and fluoride glasses, *J. Non-Cryst. Solids*, 1989, **109**(1), 35–39, DOI: [10.1016/0022-3093\(89\)90438-9](https://doi.org/10.1016/0022-3093(89)90438-9).
- 40 P. P. Pawar, S. R. Munishwar and R. S. Gedam, Eu_2O_3 doped bright orange-red luminescent lithium alumino-borate glasses for solid state lighting, *J. Lumin.*, 2018, **200**, 216–224, DOI: [10.1016/j.jlumin.2018.04.026](https://doi.org/10.1016/j.jlumin.2018.04.026).
- 41 M. Fockele, J. F. Ahlers, F. Lohse, J.-M. Spaeth and R. H. Bartram, Optical properties of atomic thallium centers in alkali halides, *J. Phys. C: Solid State Phys.*, 1985, **18**(9), 1963–1974, DOI: [10.1088/0022-3719/18/9/029](https://doi.org/10.1088/0022-3719/18/9/029).
- 42 N. Vijaya, K. Upendra Kumar and C. K. Jayasankar, Dy^{3+} -doped zinc fluorophosphate glasses for white luminescence applications, *Spectrochim. Acta, Part A*, 2013, **113**, 145–153, DOI: [10.1016/j.saa.2013.04.036](https://doi.org/10.1016/j.saa.2013.04.036).
- 43 B. Di Bartolo, *Optical Interactions in Solids*, Wiley, New York, 1968, Ch. 18.
- 44 J. A. Jiménez, S. Lysenko, H. Liu, E. Fachini and C. R. Cabrera, Investigation of the influence of silver and tin on the luminescence of trivalent europium ions in glass, *J. Lumin.*, 2010, **130**(1), 163–167, DOI: [10.1016/j.jlumin.2009.08.007](https://doi.org/10.1016/j.jlumin.2009.08.007).